Final Report (DoE-OU04523)

1. **DoE Award number:** **DE-SC0004523**
   Recipient: University of Oklahoma, Norman, OK 73019
   Program: DoE EPSCoR

2. **Project Title:** **Interband Cascade Photovoltaic Cells**
   PI: Rui Q. Yang
   Co-PIs: Michael B. Santos, Matthew B. Johnson
   Collaborator: J. F. Klem, Sandia National Laboratories, Albuquerque, NM

3. **Date of the Report:** **September 24, 2014**
   Period Covered: 07/01/2010-06/30/2014
   Budget: $590,000

4. **Participate National Laboratory:** Sandia National Laboratories, Albuquerque, NM

5. **Brief Description (abstract) of Project Goal and Objective**

In this project, we are performing basic and applied research to systematically investigate our newly proposed interband cascade (IC) photovoltaic (PV) cells [1]. These cells follow from the great success of infrared IC lasers [2-3] that pioneered the use of quantum-engineered IC structures. This quantum-engineered approach will enable PV cells to efficiently convert infrared radiation from the sun or other heat source, to electricity. Such cells will have important applications for more efficient use of solar energy, waste-heat recovery, and power beaming in combination with mid-infrared lasers. The objectives of our investigations are to: achieve extensive understanding of the fundamental aspects of the proposed PV structures, develop the necessary knowledge for making such IC PV cells, and demonstrate prototype working PV cells. This research will focus on IC PV structures and their segments for utilizing infrared radiation with wavelengths from 2 to 5 μm, a range well suited for emission by heat sources (1,000-2,000 K) that are widely available from combustion systems. The long-term goal of this project is to push PV technology to longer wavelengths, allowing for relatively low-temperature thermal sources. Our investigations address material quality, electrical and optical properties, and their interplay for the different regions of an IC PV structure. The tasks involve: design, modeling and optimization of IC PV structures, molecular beam epitaxial growth of PV structures and relevant segments, material characterization, prototype device fabrication and testing. At the end of this program, we expect to generate new cutting-edge knowledge in the design and understanding of quantum-engineered semiconductor structures, and demonstrate the concepts for IC PV devices with high conversion efficiencies.

6. **Accomplishments and Significance**

Highlights:

- Demonstrated the operation of IC PV devices at room temperature and above with a high open-circuit voltage that exceeded the single bandgap determined limit.
- Demonstrated the conversion of long-wavelength radiant photons into electricity with narrow bandgap semiconductors (*e.g.* 0.23 eV corresponding to a cutoff wavelength exceeding 5.3 μm), which would enable an attractive technology that converts the otherwise-wasted radiant energy from a heat source into useful electrical energy.

- Developed a theoretical framework for multiple stage IC PV devices, based on which the power efficiency improvement of ICPV devices are projected.
- Demonstrated the feasibility of achieving current matching between stages in ICPV devices.

Some details of these accomplishments are provided below.

An IC structure with seven identical cascade stages was designed for PV operation [4-5]. Each stage was composed of a 0.15-μm-thick 33-period InAs/GaSb SL absorber sandwiched between an AlSb/GaSb QW electron barrier and an InAs/Al(In)Sb QW hole barrier. The zero-bias spectral quantum efficiency (QE) for an ICPV device at 300 and 340 K is shown in Fig. 1. The cutoff wavelength for this device is about 5 μm at 300 K and 5.2 μm at 340 K, corresponding to bandgaps of 0.248 eV and 0.238 eV, respectively. The inset to Fig. 1 shows the electroluminescence (EL) spectra at these two temperatures. The bandgap values obtained from EL are in good agreement with the cutoff wavelengths. The QE value is relatively low due to the ~31% reflection loss from the air/semiconductor interface and the rather short overall absorber thickness (~1.1 μm total from the seven stages), which only absorbs part of the incident light. This allowed a significant amount of incident light to be transmitted to and absorbed in the ~150-μm-thick substrate. A portion of that light is reflected back from the interface between the substrate and metal sub-mount as evidenced by the somewhat strong, high-frequency interference oscillations observed in the QE curves. The value of QE was increased at the higher device temperature due to the bandgap narrowing, confirming the efficient photocarrier collection associated with the use of the short-discrete-absorber architecture in ICPV devices.

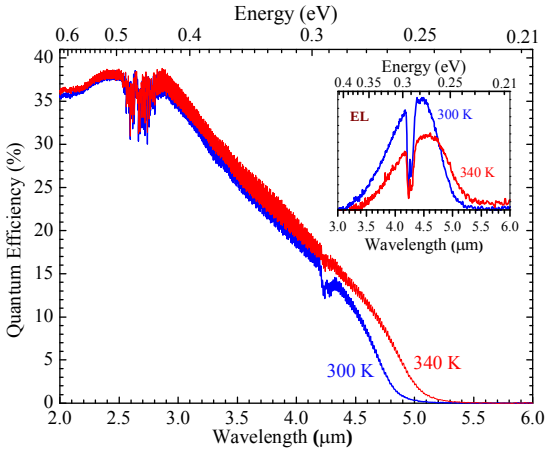

Fig. 1. Spectral QE of a device at 300 and 340 K. The inset shows the corresponding EL spectra.

Under illumination by a laser near 4.3 μm with the emission photon energy (~0.29 eV) slightly higher than the absorber bandgap, ICPV devices were able to achieve a high open-circuit voltage at 300 K and above. The intensity level from the laser on the PV devices is similar to a concentrated solar source (up to ~190 suns) with a bandwidth of ~100 nm (emission spectrum is shown in the inset to Fig. 2). The observed current density-voltage (*J*-*V*) characteristics for a 0.2×0.2 mm^2 device at 300 K and 340 K are shown in Fig. 2. The open-circuit voltage V_{oc} is as high as 0.65 V (with J_{sc}=1.4 A/cm^2), which is larger than a single bandgap determined value

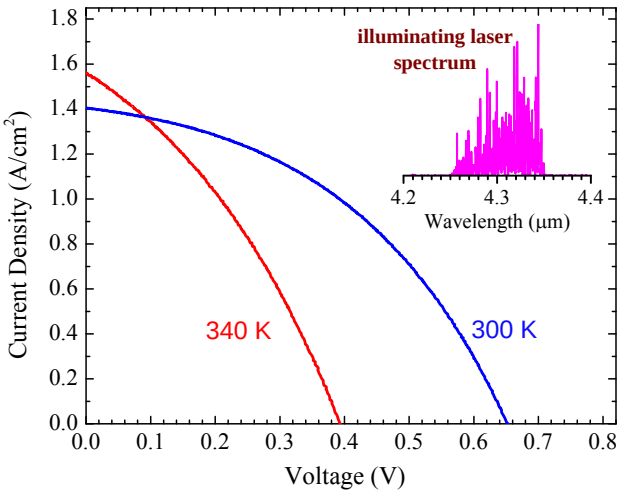

Fig. 2. Current density – voltage (*J*-*V*) characteristics of an ICPV device at 300 and 340 K under illumination by a laser with emission wavelengths near 4.3 μm (inset).

(E_g/e~0.25 V), validating the successful operation of multiple stages in series with significantly enhanced output voltage. At 340 K, the open-circuit voltage was still near 0.4 V with a cutoff wavelength near 5.2 μm and the short-circuit current density J_{sc} is higher due to the higher absorption coefficient at the same wavelength (4.3 μm) caused by the reduction in bandgap.

From the *J-V* characteristics, the extracted maximum output power density P_{max} is 395 mW/cm^2 with a fill factor (FF) of 43% at 300 K, which is smaller than a typical value (60-70%) for TPV cells with absorbers having a bandgap of 0.5-0.6 eV. This relatively low FF is partially due to the much narrower bandgap (<0.25 eV) and low QE (~15% at 4.3 μm from Fig. 1) with a thin total absorber layer (~1.1 μm). It is also possibly due to surface leakage current associated with imperfect passivation. For the same reasons, P_{max} was limited at an incident laser power density of 18.9 W/cm^2, resulting in a power efficiency of 2.1%. The voltage efficiency $eV_{oc}/(7E_g)$ is ~37%, which ultimately sets the power efficiency limit that a PV cell can achieve. An antireflection coating and more stages with the thicker overall absorber would potentially raise the QE from 15% to 80% and the power conversion efficiency to more than 10%, which would be remarkable for a low source temperature TPV system operating at such a long wavelength and with modest light intensities.

Two subsequent ICPV devices, comprising 2 or 3 stages with varied absorber thicknesses (~0.57-0.74 μm) across each structure, were investigated in order to examine the photocurrent matching between stages [6-8]. Current density vs. voltage (*J-V*) curves for two-stage and three-stage devices, each with 300×300 μm^2 square mesas, are shown in Fig. 3 for temperatures of 300 K and 340 K, obtained under illumination from an IC laser with a photon energy slightly above (within k_BT) the absorber bandgap (~0.41 eV at 300 K). The inset shows the emission spectrum of the laser used for the characterization compared to the EL spectrum of the PV device. Both the laser spectrum and the EL spectrum of the PV device peak near ~0.42 eV.

The three-stage device was able to achieve higher values of open-circuit voltage (V_{oc}) than the two-stage device, as expected. However, the short-circuit current density (J_{sc}) value was ~16% lower in the three-stage device, indicative of some mismatch of photocurrent between the different stages. There were similar differences in the J_{sc} values obtained under blackbody illumination for the two- and three-stage

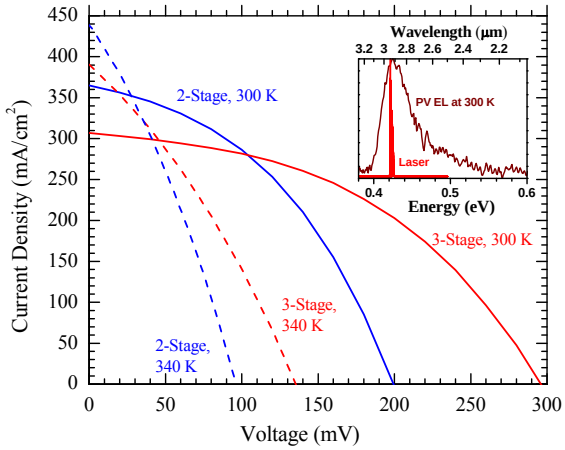

Fig. 3. Measured *J-V* curves of two-stage and three-stage devices. Both devices had 300×300 μm^2 square mesas. The inset shows the EL spectrum of the PV device at 300 K and the emission spectrum of the IC laser.

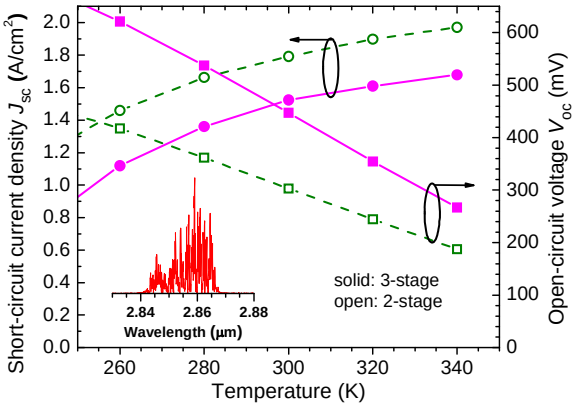

Fig. 4. J_{sc} (circles) and V_{oc} (squares) for two- and three-stage ICPV devices (0.2×0.2 mm^2) under IC laser illumination at different temperatures. Inset shows the emission spectrum for the IC laser used for these measurements.

devices. This suggests that better performance of the three-stage device should be possible simply by adjusting individual absorber thicknesses for the photocurrent matching between the stages. Nevertheless, the photocurrent matching was good enough for the three-stage devices to achieve higher output power under equivalent illumination conditions. Under laser illumination, the three-stage device had J_{sc} = 310 mA/cm^2 and V_{oc} = 295 mV. This V_{oc} value is comparable to those of the GaSb-based PV devices reported in Ref. 9. Those values ranged from 239 to 313 mV for absorbers with bandgaps of 0.50-0.55 eV. In addition, the data for the GaSb-based devices was acquired under a much higher incident light intensity (the reported J_{sc} is 3.5 A/cm^2 [9], which is about an order of magnitude higher than that of our devices). When the laser intensity was increased (to ~8 W/cm^2) on ICPV devices, the open-circuit voltage V_{oc} reached to 447 mV for a 0.2×0.2 mm^2 three-stage device at J_{sc}=1.5 A/cm^2 at 300 K as shown in Fig. 4. This again validates the advantage of the discrete cascade absorber architecture. Additionally, the photocurrent observed from these devices increased with temperature up to 350 K as shown in Fig. 4 and Fig. 5, while the diffusion length decreases with temperature. This suggests that ICPV devices indeed have efficient collection of photo-generated carriers over a large temperature range.

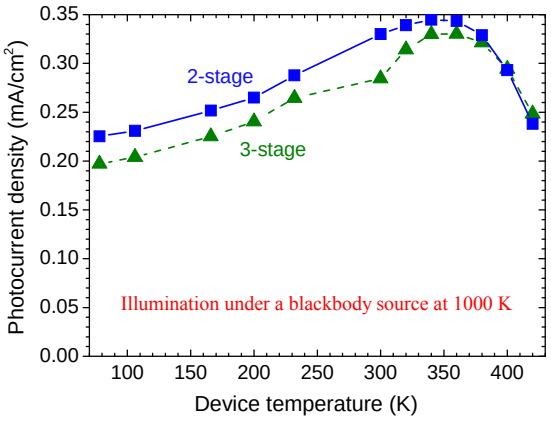

Fig. 5. Photocurrent density for 2-stage and 3-stage ICPV devices under illumination from a blackbody source at 1000 K.

At 300 K, the extracted internal QE (number of photogenerated carriers collected in all stages per an incident photon) near the laser emission wavelength is about 25% and 19% for the three- and two-stage ICPV devices, resulting in a power conversion efficiency of ~4.0 % and ~ 3.1 %, respectively. Although measured at a lower light intensity (8 vs. 19 W/cm^2), these values of the power efficiency are higher than for the previous 7-stage long-cutoff-wavelength ICPV devices because of their overall thicker absorbers and the somewhat wider bandgap. It should be noted that the devices with smaller size (0.2×0.2 mm^2) had a larger leakage current (>60%) as determined by the size-dependent product of resistance and area [7]. Hence, with more stages and antireflection coating for QE near 80% or higher, and improved passivation and device fabrication to eliminate leakage current, a power conversion efficiency approaching or even exceeding 30% is feasible in ICPV devices with cutoff wavelengths between 2 to 4 μm and better current matching. Better current matching can be achieved by simply adjusting individual absorber thicknesses and the number of cascade stages. This has been demonstrated recently by us on two long cutoff-wavelength (>5 μm) ICPV device structures, which comprised 2 or 3 stages with varied InAs/GaSb absorber thicknesses (~0.61-0.94 μm) across each structure [8, 10]. Fig. 6 shows plots of V_{oc} and J_{sc} for the two- and three-stage devices (with illumination of a laser) at different temperatures. The photocurrent density for the two devices with different stages is roughly equal under the same level of light illumination. The monotonic decrease in the V_{oc} values with increasing temperature was mainly caused by the higher dark current and shorter carrier lifetime at higher temperatures. Fig. 6 also indicates that the short-circuit current density increased from T=150 K to T=300 K for both devices and decreased at T=340 K. The rise of photocurrents with temperature was due to the increased absorption of photons as the bandgap decreased with increasing temperature. The decreasing photocurrent at the high

temperature (i.e. 340 K) may be caused by the reduction of the diffusion length. *J-V* characteristics were close to the ideal situation at low temperatures as shown by the inset to Fig. 6 when the dark current density was negligible. The *J-V* shape is essentially unchanged with different number of cascade stages, which suggests a negligible series resistance between stages.

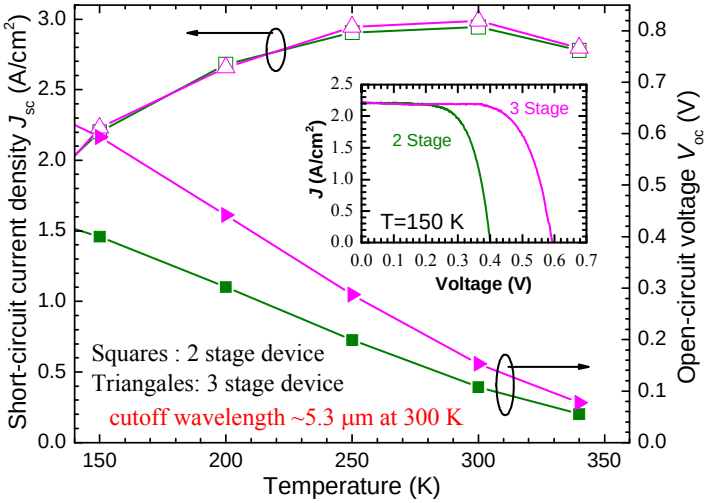

Fig. 6. Short-circuit current density J_{sc} and open-circuit voltage V_{oc} for two- and three-stage devices at different temperatures. The inset shows their current density – voltage characteristics at 150 K.

The proof-of-principle demonstrations of the ICPV concept are a significant milestone. However, they also highlight the materials challenges that must be overcome for widespread application of this technology. Our highest power conversion efficiency is ~ 4% for illumination at ~2.9 μm. For narrow bandgap materials with a cutoff wavelength near 5 μm, the dark current density is quite high. For a cutoff of 2 to 4 μm, we estimate that an antireflection coating, better current matching with more stages, as well as improved device passivation, would potentially raise the quantum efficiency to 80% and the power conversion efficiency to more than 20%, which would fulfill the requirements for certain thermophotovoltaic (TPV) systems operating at an extended wavelength spectrum and with modest concentrated light intensities. Achievement of a power efficiency of 30% will require advances in other materials aspects such as the optimization of the design of layer structures, and the further reduction of dark current through improved epitaxial materials and better device fabrication.

References

[1] R. Q. Yang, Z. Tian, J. F. Klem, T. D. Mishima, M. B. Santos, and M. B. Johnson, "Interband cascade photovoltaic devices", Appl. Phys. Lett. **96**, 063504 (2010).

[2] R. Q. Yang, "Infrared laser based on intersubband transitions in quantum wells," at *7th Inter. Conf. on Superlattices, Microstructures and Microdevices*, Banff, Canada, August, 1994; Superlattices and Microstructures, **17**, 77-83, 1995; "Novel Concepts and Structures for Infrared Lasers", Chap. 2, in *Long Wavelength Infrared Emitters Based on Quantum Wells and Superlattices*, edited by M. Helm (Gordon & Breach Pub., Singapore, 2000); "Interband Cascade Lasers", Chap. 12, in *Semiconductor lasers: fundamentals and applications*, edited by A. Baranov and E. Tournie (Woodhead Publishing Limited, Cambridge, UK, 2013); and references therein.

[3] I. Vurgaftman, W. W. Bewley, C. L. Canedy, C. S. Kim, M. Kim, C. D. Merritt, J. Abell, J.R. Lindle, and J. R. Meyer, "Rebalancing of internally generated carriers for mid-infrared interband cascade lasers with very low power consumption", *Nature Commun.*, **2**, 585 (2011).

[4] R. T. Hinkey, Z. Tian, S.M. S. Rassel, R. Q. Yang, J. F. Klem, and M. B. Johnson, "Interband cascade photovoltaic devices for conversion of mid-IR radiation," IEEE J. Photovolt. **3**, 745 (2013).
[5] H. Lotfi, R. T. Hinkey, L. Li, R. Q. Yang, J. F. Klem, and M. B. Johnson, "Narrow-bandgap photovoltaic devices operating at room temperature and above with high open-circuit voltage," Appl. Phys. Lett. **102**, 211103 (2013).
[6] R. T. Hinkey, H. Lotfi, L, Lu, R. Q. Yang, J. F. Klem, J. C. Keay, M. B. Johnson, "Interband cascade thermophotovoltaic devices with type-II superlattice absorbers of ~0.4 eV bandgap," at 39th IEEE Photovoltaic Specialists Conference, Tampa, FL, June 16-21, 2013.
[7] H. Lotfi, R. T. Hinkey, L. Li, R. Q. Yang, J F. Klem, J. C. Keay, and M. B. Johnson, "Multi-Stage Photovoltaic Devices with a Cutoff Wavelength of ~3 μm," The 40th IEEE Photovoltaic Specialists Conference, Denver, CO, June 8-13, 2014.
[8] R. Q. Yang, H. Lotfi, L. Li, R. T. Hinkey, H. Ye, J. F. Klem, L. Lei; T. D. Mishima, J. C. Keay, M. B. Santos, M. B. Johnson, "Quantum-engineered interband cascade photovoltaic devices", *Proc. SPIE*. **8993**, 899310 (2014).
[9] C. A. Wang, H. K. Choi, S. L. Ransom, G. W. Charache, L. R. Danielson, and D. M. Depoy, "High-quantum-efficiency 0.5 eV GaInAsSb/GaSb thermophotovoltaic devices." *Appl. Phys. Lett.*, **75**, 1305 (1999).
[10] H. Ye, H. Lotfi, L. Li, R. T. Hinkey, R. Q. Yang**,** L. Lei, M. B. Johnson, T.D. Mishima, and M. B. Santos, "Multistage interband cascade photovoltaic devices with a bandgap of ~0.23 eV operating above room temperature," Chinese Science Bulletin **59**, 950 (2014).

7. List of Papers

In Refereed Technical Journals

- R. T. Hinkey, Z. Tian, S.M. S. Rassel, R. Q. Yang, J. F. Klem, and M. B. Johnson, "Interband cascade photovoltaic devices for conversion of mid-IR radiation," IEEE J. Photovolt. **3**, 745 (2013).
- H. Lotfi, R. T. Hinkey, L. Li, R. Q. Yang, J. F. Klem, and M. B. Johnson, "Narrow-bandgap photovoltaic devices operating at room temperature and above with high open-circuit voltage," Appl. Phys. Lett. **102**, 211103 (2013).
- R. T. Hinkey, R. Q. Yang, "Theory of Multiple-Stage Interband Photovoltaic Devices and Ultimate Performance Limit Comparison of Multiple-Stage and Single-Stage Interband Infrared Detectors", J. Appl. Phys. **114**, 104506 (2013).
- H. Ye, H. Lotfi, L. Li, R. T. Hinkey, R. Q. Yang**,** L. Lei, M. B. Johnson, T.D. Mishima, and M. B. Santos, "Multistage interband cascade photovoltaic devices with a bandgap of ~0.23 eV operating above room temperature," Chinese Science Bulletin **59**, 950 (2014).
- R. T. Hinkey, R. Q. Yang, "Theoretical Comparison of Performance Limits of Single- and Multiple-Stage Photovoltaic Devices", (submitted 2014).
- H. Lotfi, R. T. Hinkey, L. Li, R. Q. Yang, J. F. Klem, J. C. Keay, M. B. Johnson, *et al*. "Multi-Stage Interband Cascade Photovoltaic Devices" (in preparation to be submitted).

In Conference Proceedings or/and Presentations

- L. Li, J. C. Keay, H. Ye, T. D. Mishima, Z. Tian, R. Q. Yang, M. B. Santos, M. B. Johnson, "Suppression of Slip-Line Defect Formation in GaSb Substrates during Thermal Desorption of Oxide Layers", 28th North American Molecular Beam Epitaxy Conference, Aug. 14-17, 2011, La Jolla, CA.

- Z. Tian, R. T. Hinkey, R. Q. Yang, J. F. Klem, M. B. Johnson, "Mid-IR photovoltaic devices based on interband cascade structures", Paper # 443 at The 38th IEEE Photovoltaic Specialists Conference, Austin, Texas, June 3-8, 2012.
- R. T. Hinkey, H. Lotfi, L, Lu, R. Q. Yang, J. F. Klem, J. C. Keay, M. B. Johnson, "Interband cascade thermophotovoltaic devices with type-II superlattice absorbers of ~0.4 eV bandgap," at 39th IEEE Photovoltaic Specialists Conference, Tampa, FL, June 16-21, 2013.
- H. Ye, H. Lotfi, L. Li, R. T. Hinkey, R. Q. Yang, L. Lei, J. C. Keay, M. B. Johnson, and M. B. Santos, "Interband cascade photovoltaic devices operating at room temperature and above with a bandgap of ~0.23 eV", The 16th International Conference on Narrow Gap Semiconductors, Hangzhou, China, Aug. 2-5, 2013.
- Rui Q. Yang, Hossein Lotfi, Lu Li, Robert T. Hinkey, Hao Ye, John F. Klem, L. Lei, T. D. Mishima, J. C. Keay, M. B. Santos, M. B. Johnson, "Quantum-engineered interband cascade photovoltaic devices" (**invited**), Quantum Sensing and Nanophotonic Devices XI at Photonics West, San Francisco, CA, Feb. 2-6, 2014. (in *Proc. SPIE*. **8993**, 899310)
- H. Lotfi, R. T. Hinkey, L. Li, R. Q. Yang, J F. Klem, J. C. Keay, and M. B. Johnson, "Multi-Stage Photovoltaic Devices with a Cutoff Wavelength of ~3 μm," The 40th IEEE Photovoltaic Specialists Conference, Denver, CO, June 8-13, 2014.
- R. Q. Yang, M. B. Santos, M. B. Johnson, J. F. Klem, *et al*. "Interband Cascade Photovoltaic Cells", Physical Behavior of Materials Contractors Meeting, April 14-17, 2013, Bolger Center, Potomac, MD.
- R. Q. Yang, M. B. Santos, M. B. Johnson, J. F. Klem, "Interband Cascade Photovoltaic Cells", Physical Behavior of Materials Contractors Meeting, March 6-9, 2011, Airlie Conference Center, Warrenton, VA.

8. Other People who contributed on the project

Robert Hinkey (to 12/2013): a graduate student who was partially supported by this project (50%). He was working on device physics and device characterization. He graduated in December of 2013 and received his Ph. D degree, who is now working at Naval Research Laboratory.

Zhaobing Tian (to 3/2012): a postdoc who was supported by other projects. He was mainly responsible for device fabrication and testing. His travel to Sandia for using their facilities was supported by this project.

Tetsuya Mishima (a research scientist who is supported by OU and other projects. He helped with MBE growth).

Lu Li (10/2010-): a postdoc who was partially supported by this project (65%). He was mainly working on MBE growth, material characterization, and device fabrication.

Joel C. Keay (a research scientist who was supported by OU and other projects. He helped with MBE growth and material characterization).

Hao Li: a graduate student who was partially supported by this project (50%). She was working on MBE growth, material characterization, and aspects of the device testing.

Hossein Lotfi (08/2012-): a graduate student who was partially supported by this project (50%). He was mainly working on the device characterization and modeling.

S.M. S. Rassel: a graduate student who was partially supported by this project (20%). He was mainly working on the device fabrication and characterization.

Lin Lei (06/2013-): a graduate student who was partially supported by this project (20%). He was mainly working on the device characterization.

Yuchao Jiang: a graduate student who was partially supported by this project (15%). He was mainly helping on the device characterization and modeling.

Lihua Zhao (6/2012-5/2013): a postdoc who was partially supported by this project (10%). He was mainly helping on material characterization and device packaging.

C. Niu (8/2012-4/2013): a graduate student who was partially supported by this project (10%). He was mainly helping on the device characterization.

9. An Update List of Other Support

- National Science Foundation (NSF), "Energy-efficient interband cascade lasers," $400,000, 06/01/2010-05/30/2013 (with Michael B. Santos and Matthew B. Johnson as Co-PIs).
- Air Force Office of Scientific Research, "Low Noise Interband Cascade Photodetectors," $300K, 05/2009-11/2011 (with Michael B. Santos and Matthew B. Johnson as Co-PIs).
- NSF-Materials Research Science and Engineering Center (MRSEC), "Center for Semiconductor Physics in Nanostructures," $7.8M, Oct 2005-Sept 2013 (Matthew Johnson, P.I., with many participants at the University of Oklahoma and additional co-PIs at the University of Arkansas).
- Air Force Office of Scientific Research (AFOSR), "Low Noise Mid-Wavelength IR Photodetectors" (06/01/2012-11/30/2013), $100K (with Michael B. Santos and Matthew B. Johnson as Co-PIs).
- National Science Foundation (NSF), "Quantum-Engineered Long-Wavelength Infrared Photodetectors", (06/01/2012-05/31/2015) $360,100 (with Michael B. Santos and Matthew B. Johnson as Co-PIs).
- National Science Foundation (NSF), "Acquisition of an Advanced Molecular Beam Epitaxy Chamber for Quantum-Engineered Structures and Devices" (08/01/2012 – 07/31/2014), $866k, with Michael B. Santos as the PI).
- DoE, "Quantum Engineered Materials for Multi-Absorber Thermophotovoltaic Cells" (pending with Michael B. Santos and Matthew B. Johnson as Co-PIs).
- AFOSR, "Carrier Transport in Semiconductor Quantum Structures" (pending).
- National Reconnaissance Office (NRO), "High Operating Temperature and High-Speed Interband Cascade Devices" (pending 02/01/2015-10/30/2015)

10. Cost Status

All fund has been spent.